International Journal of Scientific Reports
Ravelo B et al. Int J Sci Rep. 2023 Nov;9(11):366-375
http://www.sci-rep.com
pISSN 2454-2156 | eISSN 2454-2164
DOI: https://dx.doi.org/10.18203/issn.2454-2156.IntJSciRep20233166

Short Communication

COVID-19 cases prediction with negative group delays digital function

Blaise Ravelo[1], Mathieu Guerin[2]*, Habachi Bilal[2], Sylcolin Rakotonandrasana[3], Wenceslas Rahajandraibe[2]

[1]Nanjing University of Science and Technology, Nanjing, Jiangsu, China
[2]Aix-Marseille University, Marseille, France
[3]Islamic University of Madinah, Engineering college, Madinah, Saudi Arabia

Received: 10 July 2023
Revised: 21 September 2023
Accepted: 22 September 2023

***Correspondence:**
Dr. Mathieu Guerin,
E-mail: mathieu.guerin@univ-amu.fr

ABSTRACT

The negative group delay (NGD) is an uncommon function enabling to propagate arbitrary waveform signals with time-advance behavior. The counterintuitive NGD function was initially experimented for anticipating typically fast and short duration electronic signals in micro- and milli-second time scale. The application of NGD function to large time scale signal attracts more and more the attention of data processing engineer. This paper aims to investigate on the ability of NGD function to predict time- dependent social data with someday time-advances. As practical case of study, an innovative application of NGD function for predicting disease cases is treated. The digital circuit theory enabling to understand the low-pass (LP) NGD canonical TF and the characterization approach is established. It is shown in which condition the first order difference equation represents a LP-NGD circuit. Then, the design method of typical LP-NGD predictor as numerical circuit is introduced in function of the expected time-advance. The NGD predictor time-variation property is theoretically initiated. The NGD time-advance varied from -7 days to -1/2 days is investigated with deterministic data prediction processing from 5-months bi- exponential waveform data. The predicted data with time-advance of about -4 days was confirmed by analytical computation and simulation. The LP-NGD digital predictor feasibility is validated with monthly COVID-19 randomly arbitrary data by computed and virtually tested results. It was investigated with sensitivity analysis that the prediction performance is better when the input signal is smoothed enough. As expected, prediction result showing very good correlation with input data is demonstrated.

Keywords: Prediction, COVID-19, Integrated-circuit, Time-advance

INTRODUCTION

The historical disaster due to the COVID-19 pandemic disease is one of biggest challenging worldwide events of the 21st century.[1-3] The prediction of pandemic end and COVID-19 data exploitation remain an open question to the data processing expert engineers.[4-6] The national and international institutions were looked for relevant techniques enabling to predict the growth of COVID-19 patient number. To face up tosuch a societal tragedy, an innovative public health surveillance technology was introduced for a survey of user perceptions[7]. Moreover, research works were conducted to develop artificial intelligence (AI) against COVID-19 based tracing apps were developed.[8-15] Different techniques of COVID-19 predictions were initiated.[8-15] The deep framework for predicting COVID-19 is proposed using CXR- and X-ray images.[9-11] Innovative COVID-19 patient detection techniques using convolutional neural network algorithm were proposed.[14-17] The monthly and annual data prediction takes an important place in today society, not only in medical area but also in the environmental science as rainfall forecasting.[18-19] The most popular detection technique is based on deep learning models.[10-

[12,20-21] Nevertheless, the AI trustworthy in times and efficiency must be guaranteed.[12,22] In addition, the management of prediction technology vulnerability requires relevant analysis and solutions.[23] For this reason, an original prediction technique using an unfamiliar NGD function is developed in the present research work. Before affording the data prediction, it is worth to describe the state of the art about the NGD function research progress. The NGD electronic function was initially applied to predict in time-advance medical and communication signals.[24-27] In 1990s, the ability to propagate signals with NGD function in time-advance was theoretically and experimentally demonstrated in electronics engineering.[28-29] The NGD effect was identified by transfer function (TF) based on the group delay (GD) analysis. In 2000s,the NGD anticipation test was carried out by with optical visible test showing lighting on/off states and audio signals.[30-32] It was stated that the NGD effect does not contradict the causality.[28-29] The feasibility of NGD function in the time-domain was verified by analog circuit operating under microseconds (μs) and milliseconds (ms) time-advance.[30-32] However, the NGD uncommon effect is misunderstood to most of design engineers. Therefore, in 2010s, a fundamental NGD theory inspired from filter theory was initiated.[33] The innovative type of low-passive (LP) NGD function enabling classify different analog topologies was introduced.[34] But the basic analog LP-NGD topologies are not susceptible to operate with more than second scale time-advance. For this reason, more innovative family of LP-NGD numerical function was designed, implemented and tested.[35-38] In difference to analog one, the numerical NGD function is susceptible to operate with discrete data.[36-37] The ability to predict ambient temperature data with minute scale was recently demonstrated.[37-38]

This paper is organized in four sections. First, section 2 introduces the basic definition and property of NGD function. The frequency domain analysis is elaborated from NGD analog TF. The discrete NGD theory including the transient characterization is established. Then, the NGD synthesis equations and design method are formulated. The design of NGD predictor proof-of-concept (POC) dedicated to predict a typically deterministic pulse signal is examined in section 3. The design method in function of targeted predictor specifications is elaborated. Then, the prediction result is analyzed and characterized. The COVID-19 data prediction practical feasibility is discussed in section 4. After design description, the NGD predictor prototype for reduced time scale virtual experiment is implemented on STM32® microcontroller unit (MCU) board. Then, the result from predicted COVID-19 data is compared to the MATLAB© calculation. Last, section 5 is the conclusion.

DESIGN THEORY OF DISCRETE DATA PREDICTION BASED NGD FUNCTION

This section describes the LP-NGD function fundamental theory based on the TF approach from frequency and time domain characterization. The property of NGD predictor is established. The design methodology is introduced in function the targeted time-advance of predictor.

LP-NGD predictor function definition

Let us denote $x(t)$ and $y(t)$, the time-dependent input and output data, respectively. The associated general block diagram of NGD function is represented by Figure 1 A. The associated minimum and maximum input parameters are x_{min} and x_{max}, respectively. The discrete sample data are denoted by input $x_k= x(t)$ and NGD predictor output $y_k=n_k(x_k)$ depicted by Figure 1 B with the discrete time $t_k=t$ with integer k =1,2,3, …. For the discretization, the sampling frequency is denoted by $f_S=1/(t_{k+1}-t_k)$. In other word, we have $k = \lceil f_s t \rceil$ with $\lceil \cdot \rceil$ is the ceil function. As indicated by Figure 1 B, the corresponding TF z-transform is defined by $N(z)=Y(z)/X(z)$ by taking input $X(z)$ and output $Y(z)$. We assume the NGD discrete impulse response n_k shown by Figure 1 A with discrete output expressed by first order difference equation:

$$Y_{k+1} = n_2 x_{k+1} + n_1 x_k + n_0 y_k \text{ ---(1)}$$

where n_0, n_1 and n_2 are real coefficients. The associated TF is expressed by $N(z)=(n_2+n_1z)/(1-n_0z)$.

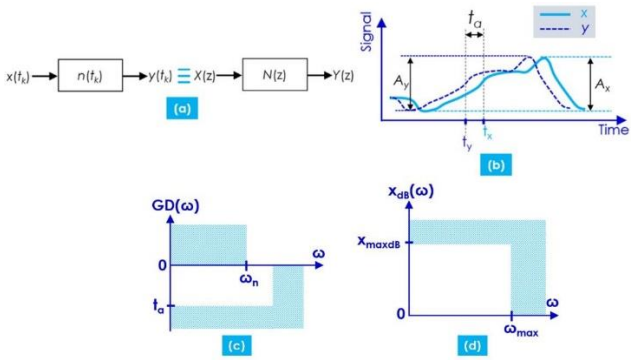

Figure 1 (A-D): NGD, discrete synoptic diagrams and ideal transient response. GD ideal response and input spectrum specification of LP-NGD predictor.

It is noteworthy that the discrete and analog symbolic variable are linked by relationship $z=\exp(j\omega/f_S)$ with angular frequency $\omega=2\pi f$. The frequency domain analysis of LP-NGD predictoris described in following subsection.

Frequency domain analysis and synthesis of the LP-NGD predictor

By denoting the Laplace $s=j\omega$, the frequency domain analysis of TF defined by $N(s)=(1+as)/(1+bs)$ where a and b are real coefficients. The associated magnitude $N(\omega)=|N(j\omega)|$ isa monotonically increasing function. The most important parameter enabling to characterize the

prediction is the GD defined by $GD(\omega)=-\partial\{\arg[N(j\omega)]\}/\partial\omega$. The considered system operates as LP-NGD function, if there is a real positive $f_n=\omega_n/(2\pi)$ named NGD cut-off frequency, $GD(\omega)\leq 0$ as illustrated by the ideal diagram of Figure 1 C. To operate with time-advance behavior, the input data $x(t)$ should be smooth enough in order to have equivalent to frequency spectrum denoted $X(\omega)=|X(j\omega)|$ with bandwidth limitation ωmax as shown by Figure 1 D. In other words, we assume that the input signal spectrum $X(\omega\leq\omega\text{max})\approx 0$. One reminds that based on the LP-NGD theory,the NGD cut-off frequency ω_n is the root of equation $GD(\omega_n)=0$.[33] At very low frequencies $\omega\approx 0$, the associated magnitude is equal to $N(\omega\approx 0)=1$. Then, the GD becomes $GD_n=GD(\omega\approx 0)$ can be written as $GD_n=b-a$. We find that this GD can be negative $GD_n<0$ for certain values of coefficients a and b. This remark implies that our TF behaves as a LP-NGD function. It can be demonstrated that the NGD cut-off frequency is given by:

$$f_n=1/(2\pi\sqrt{ab})\text{---(2)}$$

At this cut-off frequency $\omega\approx\omega_n$, the associated magnitude is equal to:

$$N(\omega_n)=\sqrt{|a|/|b|}\text{---(3)}$$

The last quantity must verify the inequality $N(\omega_n)>N(\omega\approx 0)$ because of TF magnitude N monotony. This inequality enables to forecast the integrity between the input and output spectrums because of the TF magnitude non-flatness.

NGD predictor property and synthesis

As illustrated by Figure 1 B, the NGD predictor is characterized by the time-advance $t_a\leq 0$ materialized by transient input and output relationship $y(t)\approx x(t+t_a)$. It is clear that when $t_a<0$, instead of classical positive delay effect, we have the transient signal prediction. In the transient case, by taking the test data threshold level $xT=x(t_x)=y(t_y)$ the time-advance assessment can be defined by $t_a=t_y-t_x$. Moreover, to ensure the relative error precision better than t_a+/-25%, the following condition must be fulfilled $t_a\leq -4/f_s$. As the proposed data analysis is quantitatively based on the case $x_{min}\geq 0$, the magnitude of ratio according to maximum $A_x=x_{max}$ and $A_y=y_{max}$ shown by Figure 1 B by $A=A_y/A_x$. To synthesis of NGD predictor consists in calculating the real coefficients n_0, n_1 and n_2 of difference equation (4) by solving the targeted time-advance equation $GD_n=t_a\leq 0$. In addition, for the present paper, the synthesis is based on the LP-NGD impulse response coefficient formulas recently introduced in [36] by taking the NGD cut-off frequency $f_n=-1/t_a$. It implies that for the case of LP-NGD analog function, by means of equation (10) and equation (11), we have:

$$a=-t_a\left(1+\sqrt{1+\frac{1}{\pi^2}}\right)/2\text{---(4)}$$

$$b=t_a\left(1-\sqrt{1+\frac{1}{\pi^2}}\right)/2\text{---(5)}$$

For the case of LP-NGD numerical function, the synthesis formulas are expressed as:

$$n_0=t_a f_s(\pi-\sqrt{1+\pi^2})/[\pi(2+f_s t_a)-\sqrt{1+\pi^2}]\text{---(6)}$$

$$n_1=t_a f_s(\pi+\sqrt{1+\pi^2})/[\pi(2+f_s t_a)-\sqrt{1+\pi^2}]\text{---(7)}$$

$$n_2=[\pi(2-f_s t_a)-\sqrt{1+\pi^2}\,/[\pi(2+f_s t_a)-\sqrt{1+\pi^2}]\text{---(8)}$$

The methodology to design the NGD predictor can be performed in similar way as all numerical electronic ones. The NGD predictor design method can be summarized by the following steps: Step A: Specification of targeted time-advance $t_a<0$ of the NGD predictor. Step B: Specification of sampling period $T_S=1/f_S$ and range of the considered input as the time-dependent COVID-19 data. Step C: Calculation of NGD predictor difference equation coefficients in function of input parameters t_a and T_S. Step D: Design and implementation of the NGD predictor as electronic circuit POC. Step E: Frequency domain analysis of the LP-NGD predictor in the input data spectrum and step F: Characterization of the validation experimental test showing the data prediction

By following carefully, the described method, an NGD POC is designed, implemented and tested.The following section discusses on the experimental validation results.

DETERMINISTIC PULSE SIGNAL TRANSIENT CHARACTERIZATION OF NGD PREDICTOR

The present section is aimed to the NGD predictor pre-characterization. After frequency domain analysis, the NGD predictor design function is derived from difference equation (1). As verification result, the POC is studied by means of deterministic pulse signal.

Frequency domain graphical analysis

This graphical frequency domain analysis aims to study the GD and magnitude versus time- advance t_a from minimum $t_a\text{min}$=-7 days to maximum $t_a\text{max}$=-7 days. For this spectral approach, the analysis frequency band is delimited by $f\text{min}$=0 Hz and $f\text{max}$=28 µHz. The LP-NGD analog coefficients a and b calculated from equations (4) and (5) are displayed by Figure 2 (A). The analog TF coefficients decrease linearly. The limits of the LP-NGD TF coefficients $a\text{max}$ to $a\text{min}$ and $b\text{max}$ to $b\text{min}$ expressed in minutes (mn) are recapitulated by Table 1. The GD and magnitude 2-D mapping plot variations

versus pair (t_a,f) are explained by Figure 2 B and Figure 2 C, respectively. Asseen in Figure 2 B, GD at very low frequencies $f\approx0$ are equal to the targeted t_a. Then the GD absolute value decrease with the frequency. The NGD cut-off frequency f_n belongs to the interval [$f_n$min,$f_n$max] with values indicated by Table 1. The LP-NGD function magnitude N increases with frequency especially when $|t_a|$ increases as depicted by Figure 2 C. The LP-NGD TF magnitude maximum decreases from about $N(t_a\text{min})$ to $N(t_a\text{max})$ which are indicated by Table 1. The $GD(f)<0$ variation by verying the targeted time-advance from $t_a=t_{amin}$ to $t_a=t_{amax}$ is viewed by Figure 2 D in linear plot and in Figure 2 E in semilog plot when $f<f_n$. The semilog plot of magnitude in the considered frequency band is shown by Figure 2 F. After the frequency domain analysis, it is more rigorous to reveal the NGD predictor with time-advance aspect with transient approach.

Table 1: Min and max values of analog and discrete LP-NGD predictor coefficients.

Limit	a	b	N_{max}	f_n	t_a	c_0	c_1	c_2
Min	0.5124 days	17.85 mn	17.68 dB	1.65 µHz	-7 days	0.01	-5.99	6.9
Max	7.173, days	4.152 days	32 dB	23.15 µHz	-0.5 days	0.17	-0.5	1.4

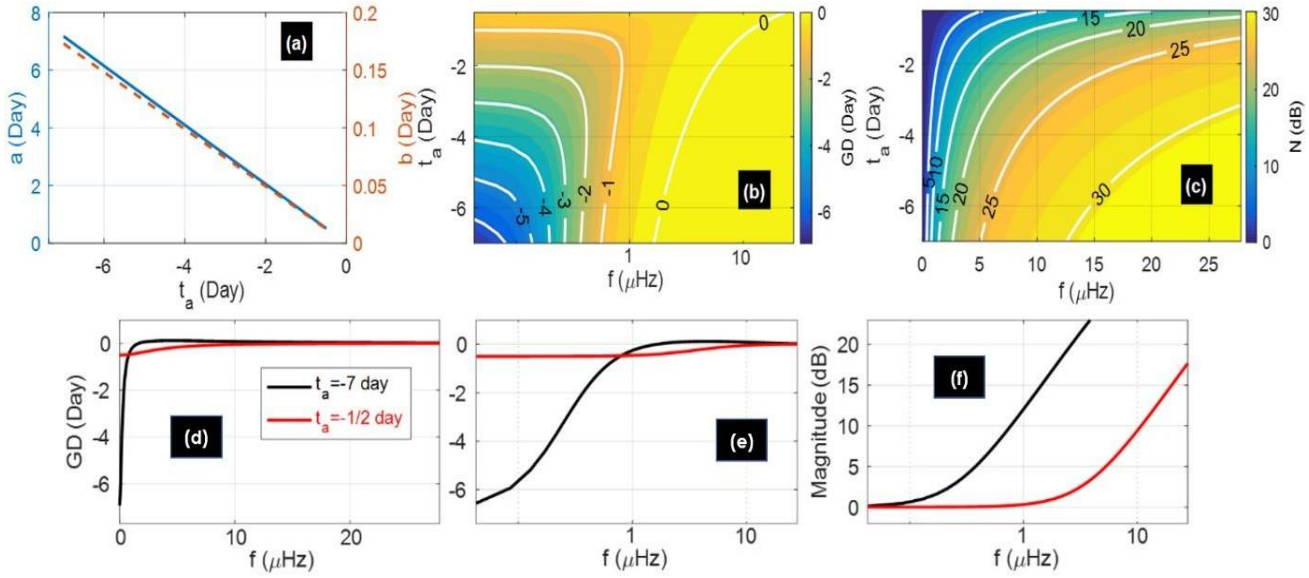

Figure 2 (A-F): LP-NGD TF, coefficients versus t_a, GD and magnitude 2-D mapping plots vs pair (t_a,f). Plots of LP-NGD TF coefficients vs ta, GD in linear, semi-log, and magnitude 1-Dplots for time-advance varied from t_{amin}=-7 day and t_{amax}=-0.5 day.

Design description of the NGD predictor

The transient characterization of the employed LP-NGD predictor for the given time-dependent input data was performed in order to extract the input-output time-advance, magnitude ratio and cross correlation introduced in Subsection 2.3. The design was carried out in MATLAB® programming environment following the proposed methodology. The simulation is based on the data operation with sampling period T_S=1 day. The considered time-advance t_a is assumed in the range from minimum t_{amin} to maximum t_{amax}. The sampling frequency corresponding to T_S=1 day is f_S=11.6 µHz. The coefficients of LP-NGD predictor difference equations are calculated from formulas (6), (7) and (8).

Figure 3 A, represents the plots of calculated NGD predictor coefficients versus t_a. We remark that coefficients $c0$ and $c2$ increases however $c1$ decreases with respect to t_a. Table 1 addresses the LP-NGD minimum and maximum coefficients in the considered t_a. The input signal x provided by the generator source is injected to the LP-NGD predictor test board. The virtual test of deterministic input was performed with driver equipped by microprocessor operating with 12-bit precision data. The test signal dynamic range is between x_{min}=0 V to ideal x_{max}=1000 and quantum resolution equal to Δx=1.

As application example, the calculated difference equation coefficients c_k=0,1,2 for three different targeted time-advances t_a={-7, -4, -1/2} days are addressed by Table 2. For the test case with t_a=-4 days, the LP-NGD predictor was coded in C-language program as indicated by Figure 3 B.

Table 2: LP-NGD predictor coefficients for COVID-19 input data. Comparison of input *x* versus output *ya*(*t*+|*ta*|) associated to the results shown by Figure 4 C. Transient characteristics of LP-NGD predictor from result shown by Figure 4 F.

Targeted t_a	-7 days	-4 days	-1/2 days
c_0	0.1475	0.09	0.0122
c_1	-6.1149	-3.7301	-0.5061
c_2	6.6974	4.6401	1.4939
15 261	276	279	283
30 714	726	754	796
45 859	857	874	904
60 637	627	622	612
75 325	316	302	275
90 120	115	102	82
105 34	32	28	18
120 7	7	6	6

LP-NGD with targeted t_a	$t_{a\uparrow}$ (days)	$T_{a\downarrow}$ (days)	A	$\zeta(x,y)$
-7 days	-6	-6	0.59 dB	94.6%
-4 days	-3	-4	0.17 dB	98.1%
-1/2 days	0	0	0 dB	99.9%

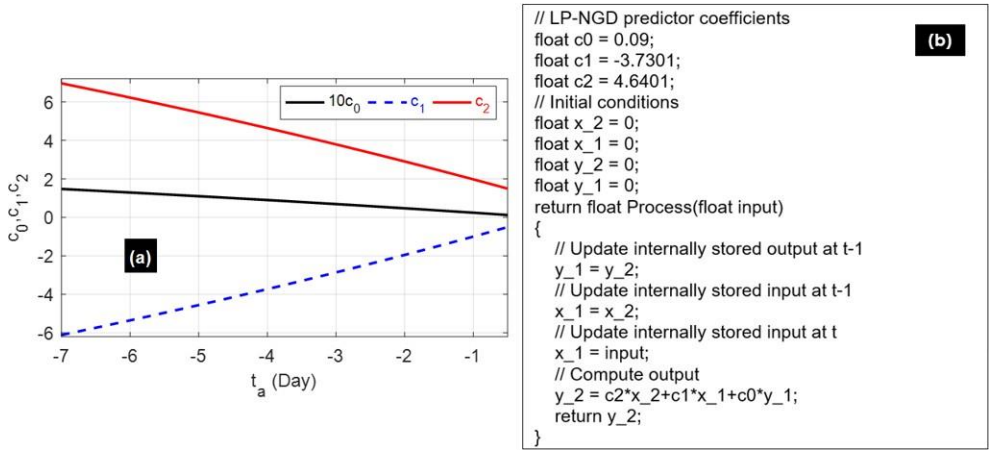

Figure 3 (A and B): LP-NGD predictor difference equation coefficients vs t_a and implemented pseudo codefor t_a=-4 days.

As initial step of the characterization, we need a deterministic pulse signal having analytic possibility to control bandwidth, magnitude and input-output rise/fall fronts.

LP-NGD predictor deterministic transient response

The initial characterization test is based on the deterministic input signal represented by bi- exponential waveform pulse voltage. The test data pulse sampled by T_S= 1 day has duration t_{max}=5months in the time interval [0, t_{max}]. The data quantity represented by input signal intentionally chosen as an asymmetrical pulse is analytically determined by: $x(t) = x_0\left[\exp\left(-\frac{t^2}{t^2}\right) - \exp\left(-\frac{t^2}{t^2}\right)\right] with\ x_0 = 10^4$ quantities $t_1 = 45\ days\ and\ t_2 = 40\ days$. We denote that the initial data is $x1$=0 and the maximal data quantity is $xmax$=x($t0$≈1.433 days)≈864 at the instant time t=$t0$. The family of input x versus pair (t,ta) for the time-advance ta varied range from $tamin$=-7 days to $tamax$=-0.5 days is displayed in the 2-D mapping of Figure 4 A. The NGD predictor output family $y(t,ta)$=$n[x(t,ta)]$ (see Figure 1A is monitored by Figure 4 B. The anticipation of the input understood by the color level shifting to the left side with respect to the desired time- advance ta. To get further insight on the relevance of the developed NGD predictor, the calculated transient results and the targeted time-advance ta={-7, -4, -1/2} days are plotted by Figure 4C. As seen in this figure, we observe successfully in blue dashed, pink solid and red dashed curves, the prediction of the bi-exponential data for the considered ta={-7, -4, -1/2} days, respectively. By comparing x and the shifted outputs y(*t*+|*ta*|), Table 2 states examples of numeric NGD predicted integer values for the different results plotted by Figure 4 C.

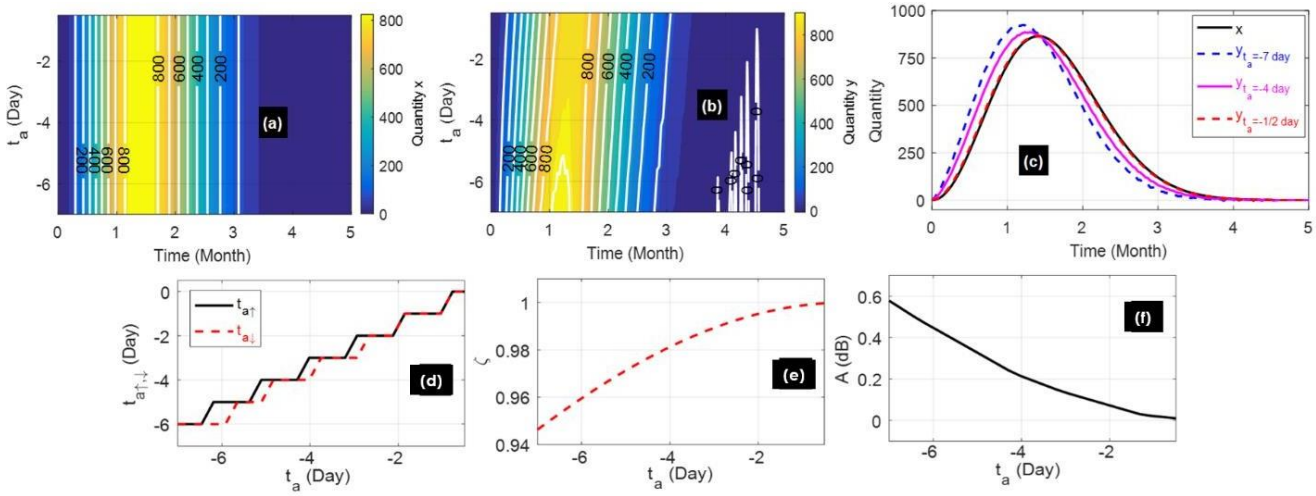

Figure 4 (A-F): 2-D mappings of bi-exponential input and output data versus pair (t_a,t), and calculatedLP-NGD predictor transient responses for the targeted t_a={-7 day, -4 day, -0.5 day}. Input-output rise and fall time-advances, cross correlation coefficient and gain from transient responses versus ideal t_a.

Transient characterization

By taking $x_T=x_{max}/2\approx432$, the rise and fall time-advances assessed from the transient results are determined from relations:

$$\begin{Bmatrix} t_{a\uparrow} = t_{y\uparrow} - t_{x\uparrow} \\ t_{a\downarrow} = t_{y\downarrow} - t_{x\downarrow} \end{Bmatrix} \text{---(9)}$$

$$\begin{Bmatrix} x(t_{x\uparrow} < t_0) = x_T = y(t_{y\uparrow} < t_0) \\ x\,(t_{x\downarrow} > t_0) = x_T = y(t_{y\downarrow} > t_0) \end{Bmatrix} \text{---(10)}$$

The computed transient rise- and fall-time-advances are plotted in solid black and dashed red curves of Figure 4 D. The discontinuity behavior is due to the fact that the time-resolution of input data x is T_S=1 day. In addition, the correlation coefficient between the input and output signals is assessed by MATLAB® function "*corrcoef*" by the relation $\zeta(x,y)=corrcoeff[x(t),y(t)]$. It is obvious that the correlation coefficient shown by Figure 4 E increases when $|t_a|$ decreases. Then, theoutput and input magnitude ratio $A(t_a)$ is plotted in Figure 4 F. The magnitude ratio decreases when $|t_a|$ decreases due to the spectrum of TF magnitude N shown by Figure 2 C. For the three cases of study, the LP-NGD predictor outputs present the counterintuitive effect of leading- and tailing- edge time advance. Table 2 indicates the quantification of the transient characterization parameters of the designed LP-NGD predictor by targeting the different time-advance t_a={-7, -4, -1/2} days. For the case t_a=-1/2 days, the assessed transient result time-advances $t_a\approx0$ day and because T_S=1 day>$|t_a|$. In addition to deterministic input signal validation, more realistic COVID-19 data plotted from several month duration is examined in the next subsection

NGD PREDICTION OF COVID-19 DATA

This section focuses on the NGD predictor test feasibility with COVID-19 data processing. The time- domain data is analyzed to extract the specific parameters. The appropriated NGD prediction is designed and implemented. The NGD predicted results with consideration of smooth average function are discussed.

COVID-19 data description

The time-domain characterization test of NGD predictor remains a challenging task. The demonstration of signal prediction with NGD function is not a familiar task for non-specialist researchers and engineers. Therefore, an easy-to-understand configuration test is proposed in the present section. The feasibility study of the developed NGD predictor is tested with medical COVID-19 data provided by Johns Hopkins Coronavirus Resource Center.[39] The test input data $x \in \mathbb{N}$ representing the number of patients corresponds substantially to arbitrary waveform signal changing randomly in time. The input data is delimited by maximum cases x_{max}<40,000 patients and initial cases x_1=2972 patients. The data presents maximal time duration t_{max}=27 months=118 weeks=810 days and the sampling period T_S=1 day. For the present case of study, the predictor is expected to operate with targeted t_a=-4 days. Emphatically, like in the previous section, we have the same NGD predictor coefficients indicated in the middle row of Table 1. The NGD predictor was design following the methodology indicated by section 2.3. The computed techniques of the NGD predictor are investigated in the following subsection.

Virtual experimentation and prediction results

To validate the developed NGD prediction, two different

techniques were considered by using realistic medical COVID-19 data.[39] The first validation technique is originally based on typical virtual measurement. The test was based on simulating the COVID-19 data driving signal generator. The synoptic diagram illustrating the interaction mechanism of the virtual test setup is depicted by Figure 5. The operation test was implemented by using the microcontroller unit (MCU) configuration including the input data convoluted to the NGD predictor TF as defined by recursive equation (2).

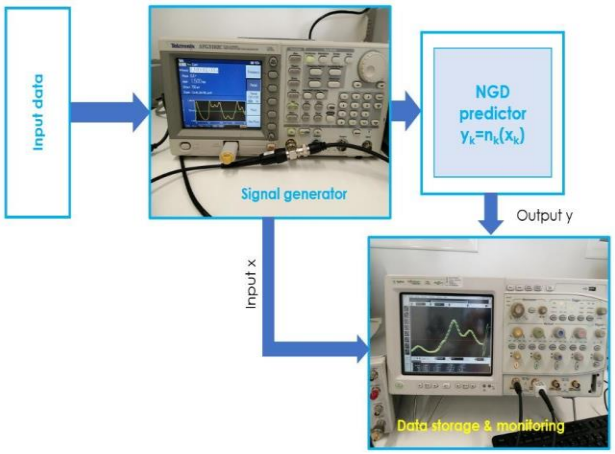

Figure 5: Illustrative diagram of virtual test configuration.

Doing this, the COVID-19 data time parameter was rescaled under time factor Tf=1/86400. Therefore, the real sampling period T_S=1 day was assumed with reduced time scale having sampling period T_{SS}=1.6534 µs. The other validation technique is the calculation from the LP-NGD analytical model $y=n(x)$ introduced earlier by means of discrete equation (4). The COVID-19 predicted results were computed following the LP-NGD predictor response routine algorithm associated to the pseudo code of Figure 3 B. The tested data storage and monitoring are recorded in csv-format and replotted in MATLAB® environment. The obtained predicted results with COVID-19 data are discussed in following subsections.

Discussion on NGD predicted results

In this case of study, the input COVID-19 raw data x is a typical arbitrary waveform signal having maximal time duration t_{max}=27 months. To perform the virtual test, we use reduced time scale factor with maximum value t_{maxS}=1.18 s. As a matter of fact, we have the screen snapshots of experimented result viewed in Figure 5. An obvious advance of output signal compared to the input is observed for the different sequences of data. By changing the measured result time scale, we can use it for comparison with the MATLAB® calculation. Figure 6 A represents the comparison of the virtual tested and calculated COVID-19 data results.

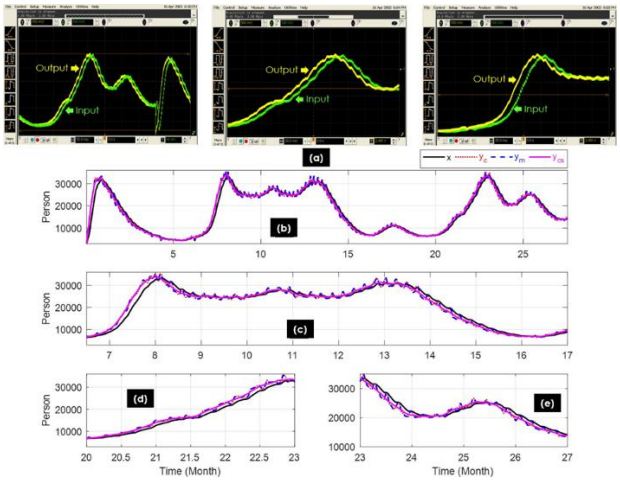

Figure 6 (A-E): Virtual test predicted viewed results with reduced scale COVID-19 data input. Comparison between the calculated and measured NGD predictor responses with COVID-19 input data: large timescale, and zoom in plots for $t \in$ TI1, $t \in$ TI2 and $t \in$ TI3.

The measured output data denoted by y_m is plotted in dashed blue curve. Then, the calculated output data denoted by y_C is plotted in red dashed line. As expected, the outputs y_m and y_C which are in very good agreement show an interesting prediction of input x. However, after result processing, the output accuracy is affected by significant with signal-to-noise ratio of about 20 dB. To filter the input signal noise effect, we generate smoothed input signal $x(k)\rightarrow x_S(k)$ by using integer $m\leq 10$ sample moving average data. The smooth pre-processing was carried out by input data by using function:

$$x_s(k,m)=\begin{cases} x(k)\ if\ x<m \\ x(k-m+1)+\cdots+x(k)]/m\ \ if\ k\geq m \end{cases} \quad \text{---(11)}$$

By taking m=7, we have the output $y_{CS}=n(x_S)$ plotted in pink solid line of Figure 6. To highlight more clearly the feasibility of the prediction, three different graphs showing more zoom in plots are displayed by Figure 6 B, Figure 6 C and Figure 6 D within the time intervals TI_1=[6.5 days, 17 days], TI_2=[20 days, 23 days] and TI_3=[23 days, 27 days], respectively. As expected, a very good prediction of COVID-19 data is observed with arbitrary waveform data anticipation. In difference to the previous NGD study delimited to some hours data analysis, the obtained temporal results illustrate the prediction of monthly slow variation. The average time-advance assessed by comparing input x and smoothed output y_{CS} is of about $t_{ac}\approx$-3.69 days. The average relative error defined by $\varepsilon_r=100|t_{ac}-t_a|/|t_a|$ is about 7.75%. Further investigation about the smoothing average effect and input-output cross correlation is examined in the next subsection.

Analysis of NGD predictor smooth responses

By using the COVID-19 input data[39] presented in the previous subsection, a parametric study of NGD predicted responses in the time-domain was performed by varying the moving smooth average parameter m from m_{min}=1 to m_{max}=10. Therefore, the calculated results are plotted in 2-D mapping versus pair (t, m) displayed by Figure 7. For the better representation visibility, the 2-D mapping analysis was performed in limited time intervals. Subsequently, the input data x are shown by Figure 7 A, B and C, represented in the zoomed-in time intervals TI_4=[0,6.5 days], TI_5=[6.5 days,16 days] and TI_6=[16 days, 27 days], respectively.

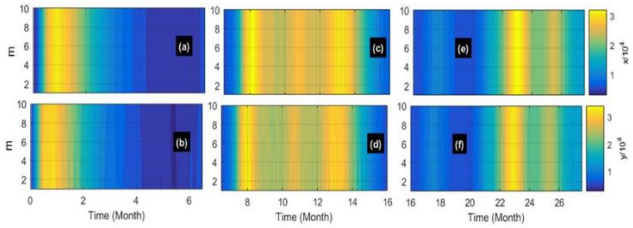

Figure 7 (A-F): 2-D mapping plots of COVID-19 data LP-NGD predictor responses: input and output for $t \epsilon$ TI4, input and output for $t \epsilon$ TI5, input and output for $t \epsilon$ TI6, versus pair (t,m).

The corresponding outputs y are viewed in Figure 7 B, D and F, respectively. It can be understood by comparing the maps of output results shown in Figure 6 A vs Figure 7 B, Figure 7 Cvs Figure 7 D, and Figure 7 E vs Figure 7 F, the prediction behavior with t_a=-4-day time-advance is better with higher value of smooth average parameter m. As expected, it can be seen that because of input noise reduction, the LP-NGD response is smooth better for m>5. Further investigation about the smoothing average effect is highlighted by Figure 8. The performance of the developedNGD predictor can be assessed by comparison of input-output cross correlation ζ.

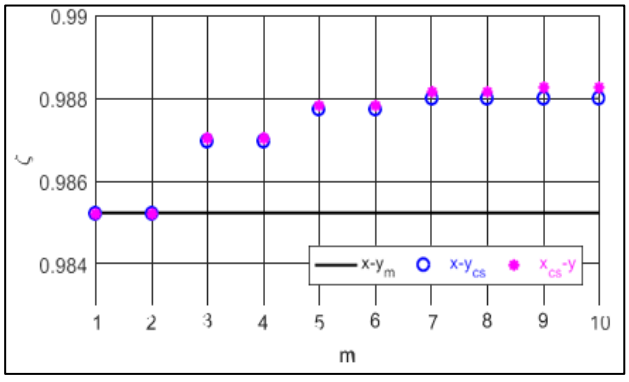

Figure 8: Comparison of cross correlation coefficients from the calculated and measured transient responses from the COVID-19 data versus smooth average number.

Moreover, the x-y_m, x-y_{CS} and x_{CS}-y cross correlation between the input and raw measured, calculated and smoothed-calculated outputs are plotted in black solid, circle-dot blue and star-dot pink curves of Figure 8, respectively. It can be pointed out that the correlation coefficient between input x and output y is improved when m increases. The output noise effect is visibly reduced when m higher than 5. The assessed cross correlations between LP-NGD predictor results shown by Figure 8 for m={1, 4, 6, 10} are $\zeta(x,y_{CS})$={98.52%, 98.69%, 98.77%, 98.77%} and $\zeta(x_{CS},y)$={98.52%, 98.70%, 98.78%, 98.78%}. We can emphasize that in this test case, the cross correlation between the input-output data is clearlyimproved better than 98% when m is increased.

CONCLUSION

An original prediction method based on NGD function is efficiently developed and applied to the COVID-19 data processing. The NGD predictor theory is established by frequency and time domain approaches. The synthesis formulas to determine the LP-NGD parameters in function of targeted time- advance are presented. The POC for validating the NGD-prediction concept is designed and studied intwo different techniques such as virtual measurement with time rescaling and MATLAB® calculation. The effectiveness of the LP-NGD predictor design is verified by two different cases of study. The first case is based on deterministic input data from analytical bi-exponential pulse signal. Relevant results showing prediction are obtained by fixing the time-advance varying from -7 days to -1/2 days. The NGD predictor performance is assessed by determining the rise/fall time-advance, magnitude ratio and cross-correlation between the input and output data. The 2nd case of study is more realistic virtual test employing medical data provided by Johns Hopkins Coronavirus resource center. The LP-NGD predictor robustness is also validated with real COVID-19 data having 27 months duration by consideringa smooth average function. It was found that prediction with -4 days' time-advance is obtained by considering smooth average function of predicted results. In the continuation of the present research work, real-time prediction of societal data is in progress. The developed NGD predictor is prominent pioneer research work for solving societal problem requiring data anticipation in environment science.

Funding: No funding sources
Conflict of interest: None declared
Ethical approval: Not required

REFERENCES

1. Chauhan S. Comprehensive review of coronavirus disease 2019 (COVID-19). Biomed J. 2020;43(4):334-40.
2. What four coronaviruses from history can tell us about COVID-19. Available at: https://www.

newscientist.com/article/mg24632800-700-what-four-coronaviruses-from-history-can-tell-us-about-covid-19. Accessed on 27, April, 2023.
3. Gomez-Barrero M, Drozdowski P, Rathgeb C, Patino J, Todisco M, Nautsch A. Biometrics in the Era of COVID-19: Challenges and Opportunities. IEEE Tran. Technol Society. 2022;3(4):307-22.
4. Charumilind S, Craven M, Lamb J, Sabow A, Wilson M. When will the COVID-19 pandemic end? an update. McKinsey and Company, Healthcare Systems and Services Practice, Nov. 2021. Available at: https://www.mckinsey.com/~/media/mckinsey/industries/healthcare%20systems%20and%20services/our%20insights/when%20will%20the%20covid%2019%20pandemic%20end/nov%202020/when-will-the- covid-19-pandemic-end-an-update-vf.pdf. Accessed on 27 April, 2023.
5. Michael K, Abbas R. What Happens to COVID-19 Data After the Pandemic? Socio-Technical Lessons. IEEE Tran. Technol Society. 2022;3(4):242-7.
6. Re-open EU. 2022. Available at: https://reopen.europa.eu/. Accessed on 27, April, 2023.
7. Hohma E, Burnell R, Corrigan CC, Luetge C. Individuality and Fairness in Public Health Surveillance Technology: A Survey of User Perceptions in Contact Tracing Apps. IEEE Tran. Technol Society. 2022;3(4):300-6.
8. Naudé W. Artificial Intelligence Against COVID-19: An Early Review, Rochester, NY, USA. 2020.
9. Fareed W, Abdul Salam A, Akram U, Alam M. Deep Framework for Predicting COVID-19 and Related Lung diseases using CXR Images. Proc. 2022 2nd Int. Conf. Digital Futures and Transformative Technologies (ICoDT2), Rawalpindi, Pakistan. 2022;1-7.
10. Kc K, Yin Z, Wu M, Wu Z. Evaluation of deep learning-based approaches for COVID-19 classification based on chest X-ray images. Signal Image Video Processing. 2021;15(5):959-66.
11. Cohen JP, Morrison P, Dao L, Roth K, Duong TQ, Ghassemi M. COVID-19 image data collection: Prospective predictions are the future. J Machine Learning Biomed Imaging. 2020;2:1-38.
12. Allahabadi H. Assessing Trustworthy AI in Times of COVID-19: Deep Learning for Predicting a Multiregional Score Conveying the Degree of Lung Compromise in COVID-19 Patients. IEEE Tran. Technol Society. 2022;3(4):272-89.
13. Naudé W. Artificial intelligence vs COVID-19: Limitations constraints and pitfalls. AI Soc. 2020;35:761-5.
A. Narin. Detection of COVID-19 Patients with Convolutional Neural Network Based Features on Multi-class X-ray Chest Images. Proc. 2020 Medical Technologies Congress (TIPTEKNO). 2020;1-4.
14. Wang L, Lin ZQ, Wong A. COVID-net: A tailored deep convolutional neural network design for detection of COVID-19 cases from chest x-ray images. Scientific Rep. 2020;10(1):1-12.
15. Shin HC, Roth HR, Gao M, Lu L, Xu Z, Nogues I et al. Deep convolutional neural networks for computer-aided detection: CNN architectures dataset characteristics and transfer learning. IEEE Tran. Med Imaging. 2016;35(5):1285-98.
16. Tan M, Le Q. Efficient net: Rethinking model scaling for convolutional neural networks. Int Conf Machine Learning. 2019;6105-14.
17. Gao L, Wei F, Yan Z, Ma J, Xia J. A study of objective prediction for summer precipitation patterns over eastern China based on a multinomial logistic regression model. Atmosphere. 2019;10(4):1-18.
18. Manandhar S, Dev S, Lee YH, Meng YS, Winkler S. A data-driven approach for accurate rainfall prediction. IEEE Tran. Geoscience and Remote Sensing. 2019;57(11):9323-31.
19. Elbagoury BM, Zaghow M, Salem ABM, Schrader T. Mobile AI Stroke Health App: A Novel Mobile Intelligent Edge Computing Engine based on Deep Learning models for Stroke Prediction Research and Industry Perspective. Proc. 2021 IEEE 20th Int. Conf. Cognitive Informatics and Cognitive Computing (ICCI*CC), Banff, AB, Canada. 2021;39-52.
20. LeCun Y, Bengio Y, Hinton G. Deep learning. Nature. 2015;521(7553):436-44 .
21. Ethics Guidelines for Trustworthy AI. 2020. Available at: https://op.europa.eu/en/publication-detail/-/publication/d3988569-0434-11ea-8c1f-01aa75ed71a1. Accessed on 25 April, 2023.
22. Robertson LJ, Munoz A, Michael K. Managing Technological Vulnerability of Urban Dwellers: Analysis, Trends, and Solutions. IEEE Tran. Technol Society. 2020;1(1):48-59.
23. Solli D, Chiao RY, Hickmann JM. Superluminal effects and negative group delays in electronics, and their applications. Phys Rev E. 2002;66(056601):1-12.
24. Hymel C, Stubbers RA, Brandt ME. Temporally Advanced Signal Detection: A Review of the Technology and Potential Applications. IEEE CAS Magazine. 2011;11(3):10-25.
25. Ravelo B, Lalléchère S, Thakur A, Saini A, Thakur P. Theory and circuit modelling of baseband and modulated signal delay compensations with low- and band-pass NGD effects. Int J Electron Commun. 2016;70(9):1122-7.
26. Voss HU. Signal prediction by anticipatory relaxation dynamics. Phys Rev E. 2016;93(3):(030201R):1-5.
27. Mitchell MW, Chiao RY. Causality and Negative Group-delays in a Simple Bandpass Amplifier. Am J Phys. 1998;66:14-9.
28. Mitchell MW, Chiao RY. Negative Group-delay and 'Fronts' in a Causal Systems: An Experiment with Very Low Frequency Bandpass Amplifiers. Phys Lett A. 1997;230:133-8.
29. Nakanishi T, Sugiyama K, Kitano M. Demonstration of Negative Group-delays in a Simple Electronic

Circuit. Am J Phys. 2002;70(11):1117-21.
30. Kitano M, Nakanishi T, Sugiyama K. Negative Group-delay and Superluminal Propagation: An Electronic Circuit Approach. IEEE J. Sel. Top. in Quantum Electron. 2003;9(1):43-51.
31. Munday JN, Henderson RH. Superluminal Time Advance of a Complex Audio Signal. Appl Phys Lett. 2004;85:503-4.
32. Ravelo B. Similitude between the NGD function and filter gain behaviours. Int J Circ Theor Appl. 2014;42(10):1016-32.
33. Ravelo B. First-order low-pass negative group delay passive topology. Electronics Letters. 2016;52(2):124-6.
34. Ravelo B. Elementary NGD IIR/FIR Systems. IJSPS. 2014;2(2):132-8
35. Ravelo B, Guerin M, Rahajandraibe W, Gies V, Rajaoarisoa L, Lalléchère S. Low-Pass NGD Numerical Function and STM32 MCU Emulation Test, IEEE Tran. Industrial Electronics. 2022;39(8):8346-55.
36. Ravelo B, Guerin M, Frnda J, Rajaoarisoa L, Rahajandraibe W. Thermal Wave Variation Anticipation under Minute Scale Time-Advance with Low-Pass NGD Digital Circuit. IEEE Access. 2022;10(1):127654-66.
37. Ravelo B, Guerin M, Rahajandraibe W, Rajaoarisoa L. All-pass NGD FIR original study for sensor failure detection application. IEEE Tran. Industrial Electronics. 2023;70(9):9561-71.
38. Johns Hopkins Coronavirus Resource Center COVID-19 data. Available at: https://coronavirus.jhu.edu/map.html. Accessed on 25 April, 2023.

Cite this article as: Ravelo B, Guerin M, Bilal H, Rakotonandrasana S, Rahajandraibe W. COVID-19 cases prediction with negative group delays digital function. Int J Sci Rep 2023;9(11):366-75.